Molecular Electronics

Deutsche Ausgabe: DOI: 10.1002/ange.201608973
Internationale Ausgabe: DOI: 10.1002/anie.201608973

Determining the Attenuation Factor in Molecular Wires Featuring Covalent and Noncovalent Tectons

Sonia Vela[+], Stefan Bauroth[+], Carmen Atienza, Agustín Molina-Ontoria, Dirk M. Guldi, and Nazario Martín**

Abstract: *Hybrid covalent/supramolecular porphyrin–fullerene structures were synthesized as highly efficient molecular wires with a remarkably low attenuation factor ($\beta = 0.07 \pm 0.01$ Å^{-1}). Hydrogen-bonding interactions and p-phenylene oligomers of different lengths are responsible for efficient electron transfer in the molecular wires.*

The design of suitably functionalized molecular wires is essential for the development of so-called molecular electronics.[1] A molecular wire is best described as a bridge that enables the rapid and efficient movement of charges over many chemical bonds. It guarantees efficient electronic coupling between the electroactive termini. The bridge/wire must exhibit an appropriate match between the donor and acceptor energy levels for charge-transfer processes in the form of charge separation and charge recombination to occur. Thus, it is important to probe the molecular-wire behavior and determine the efficiency of short- and long-range electron-transfer processes. One of the key parameters of a molecular bridge is the attenuation factor (β), which determines the magnitude of the electronic coupling between redox sites as well as the energy of the electron- (or hole-) transfer states localized at the two termini.[2,3]

Two different approaches are known for the design of efficient wire-like behavior in electron-donor–bridge–acceptor architectures. First, covalent linkages in the form of π-conjugated bridges are used to couple electron donors and acceptors.[4] Representative examples are oligo(*p*-phenylenebutadiynylene) (oPPB), oligo(*p*-phenylenevinylene) (oPPV), [2,2′]paracyclophane–oligophenylenevinylene (*p*Cp-oPPV), oligo(*p*-phenyleneethynylene) (oPPE), oligofluorene (oFl), oligothiophene, and polyporphyrins, to name a few.[5,6] In some cases, the molecular-wire-like behavior has been assessed by determining the β value in experiments. The values differ markedly between the different π-conjugated bridges and range from 0.25 A^{-1} for oPPB to 0.003 A^{-1} for oTP (oPPV: 0.01, *p*Cp-oPPV: 0.012, oPPE: 0.2, oFl: 0.09 A^{-1}).[4,5] In general, lower β values correlate with more efficient molecular-wire behavior, thus allowing the systematic analysis of a wide variety of molecular systems. Second, noncovalent means have been explored for the construction of electron-donor–acceptor assemblies, for example, electrostatic and/or hydrogen-bonding interactions. By far the most compelling, noncovalent interactions based on hydrogen bonds have been used to modulate electronic coupling between redox chromophores. One of the first examples, in which hydrogen bonds were shown to control electron transfer in bischromophoric systems of zinc(II) and iron(III) porphyrins, was reported by Therien and co-workers.[7] Also, Hirsch and co-workers reported the use of a Hamilton receptor/cyanuric acid motif to assemble metalloporphyrins with C_{60} derivatives.[8]

The wire behavior of hybrid assemblies, in which a combination of a covalent π-conjugated bridge and noncovalent hydrogen bonds constitute the binding between the redox sites, has not been addressed previously. Such an approach to hybrid wires is a tremendous challenge and is likely to provide impetus for the design of future molecular electronics.

A noncovalent C_{60}-based hybrid ensemble composed of a *p*-(2-fulleropyrrolidinyl)benzoate and a zinc porphyrin with an amidinium substituent was reported by our research groups. In complex **1a·2b**, the electron-transfer processes occurred exclusively through the hydrogen bonds of the amidinium–carboxylate bridge.[9] Inspired by this finding, we present herein a set of noncovalently associated C_{60}–*p*-phenylene oligomers, in which the π-conjugation length of the oligomers in the bridges has been systematically altered. Particularly important in the design is the coupling of C_{60} to the oligomeric bridge, in which the presence of a carboxylate as a terminus enables self-assembly with a porphyrin featuring an amidinium moiety through hydrogen bonds (Scheme 1). On the basis of this molecular design, we determined the effects of distance and the rate at which electron-transfer processes occur, as well as the molecular-wire behavior of systems based on π conjugation and hydrogen bonds. This bioinspired approach combining electron transfer through supramolecular and covalent connectivity resembles charge transport in a variety of natural processes, such as photosynthesis[10] and cellular respiration.[11]

From a synthetic perspective, asymmetric *p*-phenylene oligomers with aldehyde and carboxylic termini are the key

[*] S. Vela,[+] Dr. C. Atienza, Prof. Dr. N. Martín
Departamento de Química Orgánica I, Facultad de Químicas
Universidad Complutense de Madrid
28040 Madrid (Spain)
E-mail: nazmar@ucm.es
S. Bauroth,[+] Prof. Dr. D. M. Guldi
Department of Chemistry and Pharmacy and Interdisciplinary Center for Molecular Materials, University of Erlangen-Nuremberg
Erlandstrasse 3, 91058 Erlangen (Germany)
E-mail: dirk.guldi@fau.de
Dr. A. Molina-Ontoria, Prof. Dr. N. Martín
IMDEA-Nanociencia
C/ Faraday 9, Campus UAM, 28049 Madrid (Spain)
[+] These authors contributed equally.
Supporting information and the ORCID identification number(s) for the author(s) of this article can be found under http://dx.doi.org/10.1002/anie.201608973.

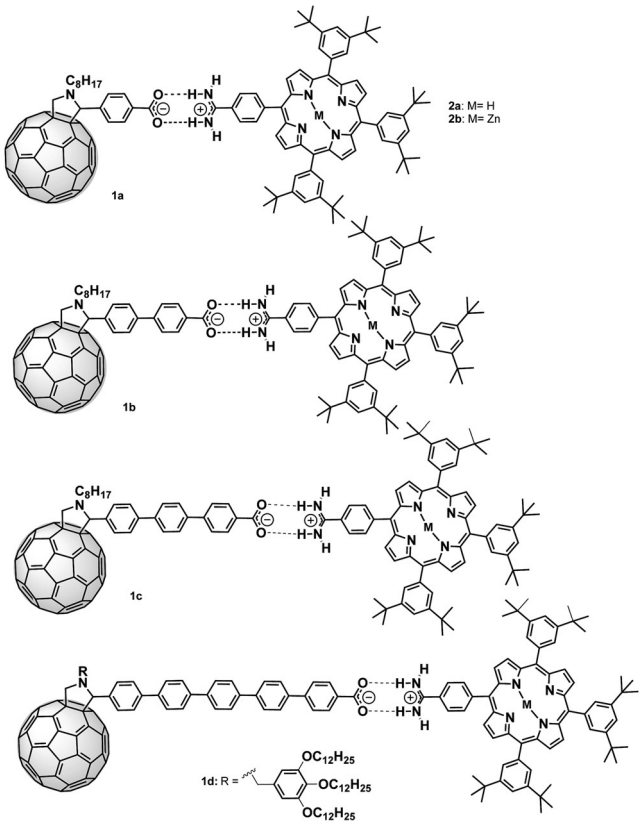

Scheme 1. Amidinium–carboxylate-based ZnP·C_{60} and H_2P·C_{60} assemblies **2a**,**b**·**1a–d**.

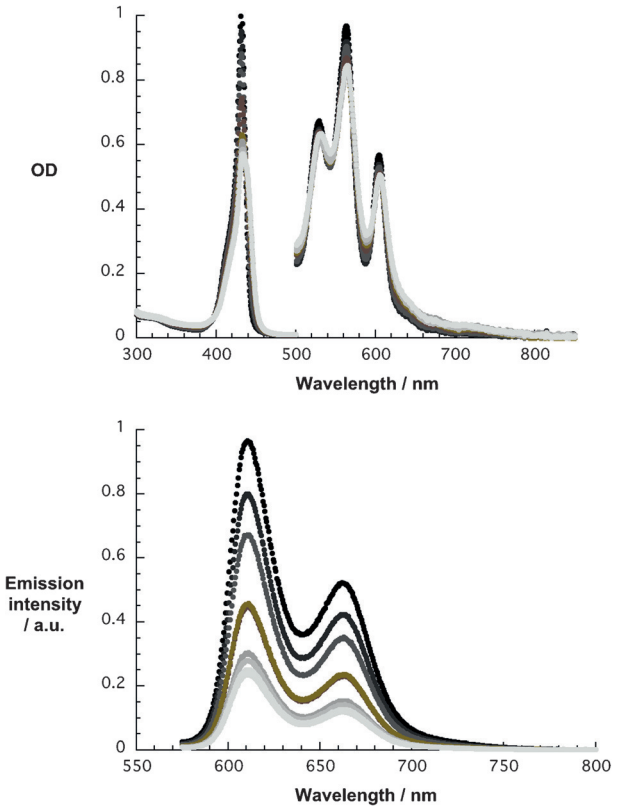

Figure 1. Top: Absorption changes observed during the complexation of **2b** (2×10^{-6} M) with **1a** (0–1.6×10^{-5} M) in toluene at room temperature. The 500–700 nm region is magnified by a factor of 20. Bottom: Normalized and fully corrected fluorescence spectra of **2b** (2×10^{-6} M) upon complexation with **1a** (0–1.6×10^{-5} M), with photoexcitation at 568 nm in toluene at room temperature.

intermediates en route to pyrrolidino[3,4:1,2][60]fullerenes **1a–d**. These oligomers were synthesized by Suzuki cross-coupling reactions between bromoaryl and organoborane compounds in the presence of a palladium(II) catalyst and a fluorine salt as a base and additive, which is crucial for the success of the cross-coupling reaction.[12] Subsequent 1,3-dipolar cycloaddition reactions were used to link the *p*-phenylene oligomers to C_{60} through a pyrrolidine ring to yield **1a–d** in high yields (see the Supporting Information for synthetic details).[13] On the other hand, **2a**,**b** were synthesized by using the conditions previously described by Ito and co-workers.[14]

Initially, we evaluated the assembly of the noncovalently bound hybrids **1a–d**:**2a**,**b** in absorption assays. Figure 1 shows, as a representative example, the spectral changes of **2b** (2×10^{-6} M) upon the addition of the C_{60} derivative **1a** (0–1.6×10^{-5} M) in toluene at room temperature. Depletion of the zinc porphyrin (ZnP) Soret and Q bands at 431, 530, 565, and 604 nm as well as bathochromically evolving transitions gave rise to eight isosbestic points. In the case of **2b** and **1a**, the emergence of a new transition at 442 nm is assigned to the formation of the complex **2b·1a**. Furthermore, for **2b·1a**, new absorptions evolved in the range between 710 and 850 nm, whereas neither **2b** nor **1a** gave rise to any appreciable features. Since **2b·1b**, **2b·1c**, and **2b·1d** lack the aforementioned absorption, we postulate, in line with previous investigations,[15] the presence of a charge-transfer state. The close spatial separation between **2b** and **1a** supports the notion of a shift of charge density from the electron donor to the electron acceptor (see Figure S1 in the Supporting Information).

To complement the aforementioned studies, we turned to steady-state fluorescence measurements of **2b** in toluene and chlorobenzene. We ensured the full disaggregation of **2b** by carrying out all experiments in the presence of 4-dimethylaminopyridine (DMAP) in a 1:1 ratio. Excitation at either 436 or 567 nm, which match the absorption of the ZnP Soret and Q band, respectively, provided insight into excited-state interactions in the presence of **1a**, **1b**, and **1c** (see Figures S2–S5).

In particular, the intensity of the ZnP-centered fluorescence (Figure 1), with maxima at 615 and 665 nm and quantum yields of 0.04, was found to depend exponentially on the concentrations of added **1a**, **1b**, and **1c**. From this observation, we infer the gradual transformation of **2b** into **2b·1a**, **2b·1b**, and **2b·1c**. The binding constants, which were obtained by nonlinear least-squares curve fitting of the ZnP fluorescence quenching integrated from 610 to 665 nm, are $(2.4\pm0.2)\times10^6$, $(1.4\pm0.3)\times10^6$, and $(1.2\pm0.3)\times10^5\,M^{-1}$ for **2b·1a**, **2b·1b**, and **2b·1c**, respectively. These values are in excellent agreement with those derived from the absorption assays (see above). Interestingly, the fluorescence quenching depends strongly on the bridge length, thus leading to

a quenching of 71, 24, and 20% for **2b·1a**, **2b·1b**, **2b·1c**, respectively (see Figures S2–S5).

Turning to the near-infrared part of the spectrum, we noted for **2b·1a** a rather broad emission between 750 and 1200 nm (see Figure S6). Deconvolution of this feature in chlorobenzene revealed ZnP-centered fluorescence and phosphorescence at around 780 and 900 nm, respectively, as well as a charge-transfer emission at 1047 nm. Excitation spectra at 800 and 1047 nm give rise to maxima at 431 and 440 nm corresponding to **2b** and **2b·1a**, respectively. The charge-transfer emission is subject to a solvent-induced redshift from 1003 nm in toluene to 1052 nm in THF, and broadening, that is, from 185 nm in toluene to 235 nm in chlorobenzene. In stark contrast, the charge-transfer emission is absent in **2b·1b**, **2b·1c**, and **2b·1d**.

Next, the corresponding ZnP·C_{60} electron-donor–acceptor hybrids were probed in transient absorption measurements in chlorobenzene upon the photoexcitation of **2b** at 430 nm. We chose the excitation wavelength of 430 nm and a 1:1:1 **2b**/DMAP/**1a–d** ratio to ensure excitation exclusively of **2b**. We started with the photoexcitation of **2b** as the ZnP reference (see Figure S7). Its singlet-excited-state features evolved, with maxima at 465, 545, 590, 645, 705, and 1300 nm and minima at 565 and 610 nm. From multiwavelength global analyses, we derived a fast S_2-to-S_1 transition within 4 ps and a first-singlet-excited-state lifetime of 1.6 ± 0.2 ns. This decay reflects the ZnP intersystem crossing, and the triplet excited state formed in this way displayed maxima at 480 and 840 nm.

For the different ZnP·C_{60} electron-donor–acceptor hybrids, the same ZnP singlet-excited-state features were discernable at early times. Notable is that the transient features were the same, but the corresponding lifetimes differed substantially. For example, in **2b·1a**, the ZnP singlet excited state decayed within 0.64 ± 0.02 ns (Figure 2), thus leading to a less efficient population of the ZnP triplet excited state. Furthermore, transient species evolved in the visible and near-infrared regions of the spectrum. However, the features of **2b·1a** were different from those of the singlet and triplet excited states of ZnP. In the visible region, maxima at 475, 595, 645, and 695 nm and minima at 570 and 615 nm resembled the features of the one-electron-oxidized form of ZnP. In the near-infrared region, a maximum at 1010 nm is a clear attribute of the one-electron-reduced form of C_{60}.

We reached the conclusion that exclusive photoexcitation of ZnP in **2b·1a** is followed by intramolecular electron transfer to afford the $(ZnP)^{\bullet+}$·$(C_{60})^{\bullet-}$ radical-ion-pair state. Considering, however, the substantial overlap of the ZnP singlet-excited-state and $(ZnP)^{\bullet+}$·$(C_{60})^{\bullet-}$ radical-ion-pair-state absorptions in the visible range, we used the ZnP singlet-excited-state absorption at 1300 nm as well as the radical-anion absorption feature of C_{60} at 1010 nm to determine the electron-transfer dynamics. The charge-separation rates were deduced as 7.9×10^{10}, 6.4×10^{10}, 3.7×10^{10}, and 2.4×10^{10} s^{-1} for **2b·1a–d**, respectively, whereas the charge-recombination rates were 1.3×10^{9}, 1.0×10^{9}, 8.7×10^{8}, and 6.0×10^{8} s^{-1}. Importantly, data deconvolution with target analysis[16,17] corroborated the charge-separation and charge-recombination trends (see Figures S8–S17).

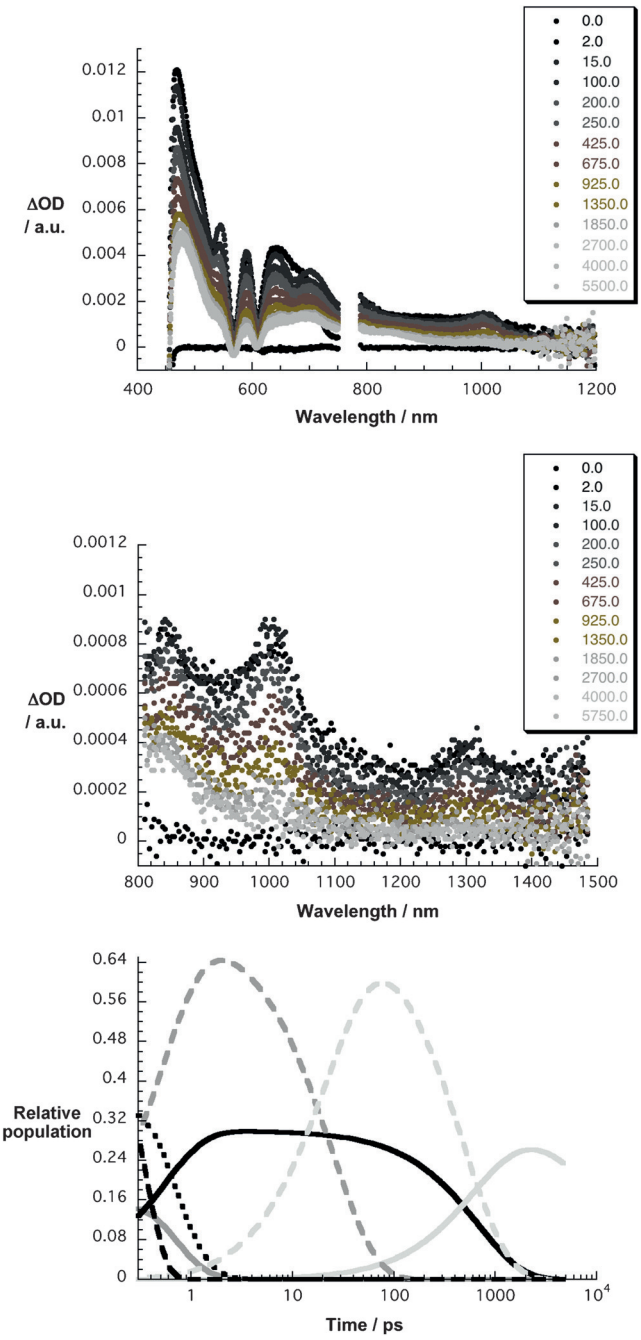

Figure 2. Top: Differential absorption spectra (visible and near-infrared) upon femtosecond flash photolysis (430 nm) of **2b·1a** in chlorobenzene at room temperature with several time delays between 0 and 5500 ps. Middle: Differential absorption spectra (extended near-infrared) upon femtosecond flash photolysis (430 nm) of **2b·1a** in chlorobenzene at room temperature with several time delays between 0 and 5750 ps. Bottom: Concentration–time profile as obtained from target analysis, showing intersystem crossing for unbound **2b** from the singlet excited state of **2b** (black solid line) to the triplet excited state of **2b** (light-gray solid line) with a rate of 1.9×10^{-9} s^{-1} and charge separation from the singlet excited state in **2b·1a** (dark-gray dashed line) to the radical-ion-pair state in·**2b·1a** (light-gray dashed line) with a rate of 7.9×10^{10} s^{-1} followed by charge recombination with a rate of 2.6×10^{9} s^{-1}.

Having established the electron rate constants, we analyzed their dependence on the electron-donor–acceptor separation, that is, the distance between ZnP and C_{60} in **2b·1a**, **2b·1b**, **2b·1c**, and **2b·1d**. From the corresponding slopes (Figure 3; see also Figures S14 and S15), β values of 0.07 ± 0.01 Å^{-1} were derived for the charge separation and charge recombination. Such low β values, especially for *p*-phenylene oligomers, are due to the induction of coplanarization between adjacent phenylene moieties by the hydrogen bonds.

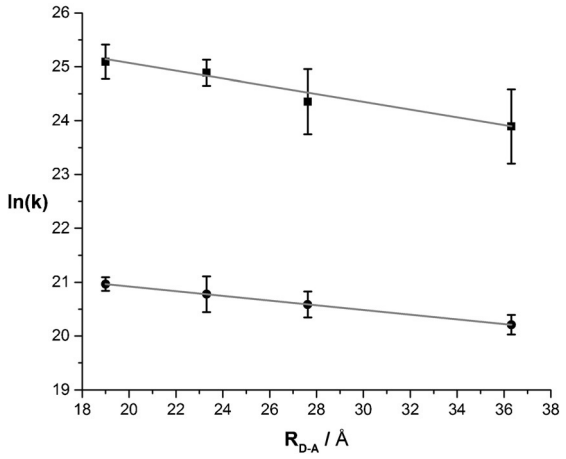

Figure 3. Dependence of charge separation and charge recombination on the center-to-edge distance in nitrogen-saturated chlorobenzene at room temperature for **2b·1a**, **2b·1b**, **2b·1c**, and **2b·1d**. The slope represents the β values.

In summary, we have carried out the systematic synthesis of a new family of electron-donating ZnP and electron-accepting C_{60} building blocks and their integration into electron-donor–acceptor assemblies. Efficient charge transport through a combination of hydrogen bonds and *p*-phenylene oligomers yielded an exceptionally small attenuation factor (β) of 0.07 ± 0.01 Å^{-1}, which is among the lowest β values reported for molecular wires. Thus, our results validate the use of hybrid covalent/noncovalent wires for molecular electronics and pave the way to future designs employing a variety of known supramolecular interactions.

Acknowledgements

This research was supported by the European Research Council (ERC-320441-Chir*all*carbon), the Ministerio de Economía y Competitividad (MINECO) of Spain (project CTQ2014-52045-R; Ramón y Cajal grant to C.A.), and the CAM (PHOTOCARBON project S2013/MIT-2841), as well as the programs "MOLESCO" and "Solar Technologies Go Hybrid". N.M. thanks the Alexander von Humboldt Foundation.

Keywords: electron transfer · fullerenes · hydrogen bonds · molecular wires · porphyrinoids

How to cite: *Angew. Chem. Int. Ed.* **2016**, *55*, 15076–15080
Angew. Chem. **2016**, *128*, 15300–15304

[1] a) A. Charisiadis, C. Stangel, V. Nikolaou, M. S. Roy, G. D. Sharma, A. G. Coutsolelos, *RSC Adv.* **2015**, *5*, 88508–88519; b) J. Sukegawa, C. Schubert, X. Zhu, H. Tsuji, D. M. Guldi, E. Nakamura, *Nat. Chem.* **2014**, *6*, 899–905; c) S. Qi, H. Iida, L. Liu, S. Irle, W. Hu, E. Yashima, *Angew. Chem. Int. Ed.* **2013**, *52*, 1049–1053; *Angew. Chem.* **2013**, *125*, 1083–1087; d) J. E. Park, M. Song, M. Hong, G. Lee, H. Choi, *Angew. Chem. Int. Ed.* **2012**, *51*, 6383–6388; *Angew. Chem.* **2012**, *124*, 6489–6494; e) S. H. Choi, B.-S. Kim, D. C. Frisbie, *Science* **2008**, *320*, 1482–1486; f) M. J. Frampton, H. L. Anderson, *Angew. Chem. Int. Ed.* **2007**, *46*, 1028–1064; *Angew. Chem.* **2007**, *119*, 1046–1083.

[2] a) C. E. Smith, S. O. Odoh, S. Ghosh, L. Gagliardi, C. J. Cramer, C. D. Frisbie, *J. Am. Chem. Soc.* **2015**, *137*, 15732–15741; b) V. Lloveras, J. Vidal-Gancedo, M. T. Figueira-Duarte, J.-F. Nierengarten, J. J. Novoa, F. Mota, N. Ventosa, C. Rovira, J. Veciana, *J. Am. Chem. Soc.* **2011**, *133*, 5818–5833; c) H. Meier, *Angew. Chem. Int. Ed.* **2009**, *48*, 3911–3913; *Angew. Chem.* **2009**, *121*, 3969–3971; d) H. U. Winters, E. Dahlstedt, H. E. Blades, C. J. Wilson, M. J. Frampton, H. L. Anderson, B. Albinsson, *J. Am. Chem. Soc.* **2007**, *129*, 4291–4297; e) M. P. Eng, B. Albinsson, *Angew. Chem. Int. Ed.* **2006**, *45*, 5626–5629; *Angew. Chem.* **2006**, *118*, 5754–5757; f) F. Giacalone, J. L. Segura, N. Martín, J. Ramey, D. M. Guldi, *Chem. Eur. J.* **2005**, *11*, 4819–4834; g) F. Giacalone, J. L. Segura, N. Martín, D. M. Guldi, *J. Am. Chem. Soc.* **2004**, *126*, 5340–5341.

[3] a) S. Izawa, K. Hashimoto, K. Tajima, *Phys. Chem. Chem. Phys.* **2012**, *14*, 16138–16142; b) A. Kira, T. Umeyama, Y. Matano, K. Yoshida, S. Isoda, J. K. Park, D. Kim, H. Imahori, *J. Am. Chem. Soc.* **2009**, *131*, 3198–3200; c) H. Imahori, *Bull. Chem. Soc. Jpn.* **2007**, *80*, 621–636; d) W. Ma, C. Yang, X. Gong, K. Lee, A. J. Heeger, *Adv. Funct. Mater.* **2005**, *15*, 1617–1622; e) G. Li, V. Shrotriya, J. Huang, Y. Yao, T. Moriarty, K. Emery, Y. Yang, *Nat. Mater.* **2005**, *4*, 865–868.

[4] a) R. Søndergaard, F. C. Krebs, *Polymer* **2011**, *3*, 545–557; b) D. M. Guldi, B. M. Illescas, C. Atienza, M. Wielopolski, N. Martin, *Chem. Soc. Rev.* **2009**, *38*, 1587–1597; c) E. A. Weiss, M. R. Wasielewski, M. A. Ratner, *Top. Curr. Chem.* **2005**, *257*, 103–133; d) T. D. K. James, J. M. Tour, *Top. Curr. Chem.* **2005**, *257*, 33–62; e) C. Schubert, J. T. Margraf, D. M. Guldi, *Chem. Soc. Rev.* **2015**, *44*, 988–998.

[5] a) T. Miura, R. Tao, S. Shibata, T. Umeyama, T. Tachikawa, H. Imahori, Y. Kobori, *J. Am. Chem. Soc.* **2016**, *138*, 5879–5885; b) K. E. Linton, M. A. Fox, L.-O. Pålsson, M. R. Bryce, *Chem. Eur. J.* **2015**, *21*, 3997–4007; c) J.-J. Shen, J. Y. Shao, Z.-L. Gong, Y.-W. Zhong, *Inorg. Chem.* **2015**, *54*, 10776–10784; d) D. Miguel, L. A. de Cienfuegos, A. Martín-Lasanta, S. P. Morcillo, L. A. Zotti, E. Leary, M. Bürkle, Y. Asai, R. Jurado, D. J. Cárdenas, G. Rubio-Bollinger, N. Agraït, J. M. Cuerva, M. T. González, *J. Am. Chem. Soc.* **2015**, *137*, 13818–13826; e) L. G. Heinz, O. Yushchenko, Y. Oleksandr, M. Neuburger, E. Vauthey, O. S. Wenger, *J. Phys. Chem. A* **2015**, *119*, 5676–5684; f) G. Sedghi, K. Sawada, L. J. Esdaile, M. Hoffmann, H. L. Anderson, D. Bethell, W. Haiss, S. J. Higgins, P. J. Nichols, *J. Am. Chem. Soc.* **2008**, *130*, 8582–8583.

[6] a) M. Wielopolski, A. Molina-Ontoria, C. Schubert, J. T. Margraf, E. Krokos, J. Kirschner, A. Gouloumis, T. Clark, D. M. Guldi, N. Martin, *J. Am. Chem. Soc.* **2013**, *135*, 10372–10381; b) S. Castellanos, A. A. Vieira, B. M. Illescas, V. Sacchetti, C. Schubert, J. Moreno, D. M. Guldi, S. Hecht, N. Martín, *Angew. Chem. Int. Ed.* **2013**, *52*, 13985–13990; *Angew. Chem.* **2013**, *125*, 14235–14240; c) A. Molina-Ontoria, M. Wielopolski, J. Gebhardt, A. Gouloumis, T. Clark, D. M. Guldi, N. Martín, *J. Am. Chem. Soc.* **2011**, *133*, 2370–2373; d) M. Wielopolski, J. Santos, B. M. Illescas, A. Ortiz, B. Insuasty, T. Bauer, T. Clark, D. M.

Guldi, N. Martín, *Energy Environ. Sci.* **2011**, *4*, 765 – 771; e) A. Molina-Ontoria, G. Fernández, M. Wielopolski, C. Atienza, L. Sánchez, A. Gouloumis, T. Clark, N. Martín, D. M. Guldi, *J. Am. Chem. Soc.* **2009**, *131*, 12218 – 12229; f) C. Atienza-Castellanos, M. Wielopolski, D. M. Guldi, C. Van der Pol, M. R. Bryce, S. Filippone, N. Martin, *Chem. Commun.* **2007**, 5164 – 5166; g) C. Atienza, N. Martín, D. M. Guldi, *Chem. Commun.* **2006**, 3202; h) D. M. Guldi, F. Giacalone, G. de la Torre, J. L. Segura, N. Martín, *Chem. Eur. J.* **2005**, *11*, 7199 – 7210.

[7] a) P. J. F. de Rege, S. A. Williams, M. J. Therien, *Science* **1995**, *269*, 1409 – 1413; b) J. L. Sessler, B. Wang, A. Harriman, *J. Am. Chem. Soc.* **1993**, *115*, 10418 – 10419.

[8] a) F. Wessendorf, B. Grimm, D. M. Guldi, A. Hirsch, *J. Am. Chem. Soc.* **2010**, *132*, 10786 – 10795; b) F. Wessendorf, J.-F. Gnichwitz, G. H. Sarova, K. Hager, U. Hartnagel, D. M. Guldi, A. Hirsch, *J. Am. Chem. Soc.* **2007**, *129*, 16057 – 16071.

[9] L. Sánchez, M. Sierra, N. Martín, A. J. Myles, T. J. Dale, J. Rebek, Jr., W. Seitz, D. M. Guldi, *Angew. Chem. Int. Ed.* **2006**, *45*, 4637 – 4641; *Angew. Chem.* **2006**, *118*, 4753 – 4757.

[10] a) M. R. Wasielewski, *J. Org. Chem.* **2006**, *71*, 5051 – 5066; b) K. N. Ferreira, T. M. Iverson, K. Maghlaoui, J. Barber, S. Iwata, *Science* **2004**, *303*, 1831 – 1838; c) R. E. Blankenship, *Molecular Mechanisms of Photosynthesis*, Blackwell Science, Oxford, **2002**.

[11] a) M. Li, S. K. Jogense, D. G. G. McMillan, L. Krzeminski, N. N. Daskalakis, R. H. Partanen, M. Tutkus, R. Tuma, D. Stamou, N. S. Hatzakis, L. J. C. Jeuken, *J. Am. Chem. Soc.* **2015**, *137*, 16055 – 16063; b) X.-H. Wang, H.-S. Peng, L. Yang, F.-T. You, F. Teng, H.-H. Hou, O. S. Wolfbeis, *Angew. Chem. Int. Ed.* **2014**, *53*, 12471 – 12475; *Angew. Chem.* **2014**, *126*, 12679 – 12683; c) T. Yamashita, G. A. Voth, *J. Am. Chem. Soc.* **2012**, *134*, 1147 – 1152.

[12] a) A. Mallagaray, A. Canales, G. Domínguez, J. Jiménez-Barbero, J. Pérez-Castells, *Chem. Commun.* **2011**, *47*, 7179 – 7181; b) S. Kotha, K. Lahiri, D. Kashinath, *Tetrahedron* **2002**, 9633 – 9695.

[13] a) E. A. Weiss, M. J. Ahrens, L. E. Sinks, A. V. Gusev, M. A. Rartner, M. R. Wasielewski, *J. Am. Chem. Soc.* **2004**, *126*, 5577 – 5584; b) B. Schlicke, P. Belser, L. de Cola, E. Sabbioni, V. Balzani, *J. Am. Chem. Soc.* **1999**, *121*, 4207 – 4214.

[14] J. Otsuki, K. Iwasaki, Y. Nakano, M. Itou, Y. Araki, O. Ito, *Chem. Eur. J.* **2004**, *10*, 3461 – 3466.

[15] D. M. Guldi, C. Luo, M. Prato, A. Troisi, F. Zerbetto, M. Scheloske, E. Dietel, W. Bauer, A. Hirsch, *J. Am. Chem. Soc.* **2001**, *123*, 9166.

[16] K. M. Mullen, I. H. M. van Stokkum, *J. Stat. Soft.* **2007**, *18*, 1 – 46.

[17] J. J. Snellenburg, S. P. Laptenok, R. Seger, K. M. Mullen, I. H. M. van Stokkum, *J. Stat. Soft.* **2012**, *49*, 1 – 22.

Received: September 13, 2016
Published online: October 28, 2016

